

THE SURFACE CHEMISTRY OF IRON FISCHER-TROPSCH CATALYSTS

D. J. DWYER AND J. H. HARDENBURGH

Exxon Research and Engineering
Corporate Research Science Laboratory
Route 22 East
Annandale NJ. 08801

INTRODUCTION

The indirect conversion of coal to liquid hydrocarbons via steam gasification followed by synthesis gas (CO/H_2) chemistry has been the subject of intensive study for a number of decades. A key technological challenge facing researchers in this area is control over the product distribution during the hydrocarbon synthesis step. In the case of iron Fischer-Tropsch catalysts, it has long been known that the addition of alkali to the metal catalyst has a significant impact on the product distribution(1). Iron catalysts treated with alkali produce less methane more alkenes and higher molecular weight products. In spite of numerous investigations (2-9), the details of this promotional effect are not understood on a molecular level. To explore the role of alkali in the surface chemistry of iron catalysts, we have carried out a combined surface science and catalytic kinetic study of a model iron catalyst with and without surface alkali.

EXPERIMENTAL

The experimental apparatus has been described elsewhere (10,11). It consists of a medium pressure microreactor coupled to a ultra-high vacuum system equipped to perform x-ray photoelectron spectroscopy. The microreactor was a small UHV compatible tube furane with an internal volume of approximately 10 cc and gold plated walls for inertness. The catalysts used in the study were pressed into a gold mesh backing material which in turn was mounted on a gold sample boat. The boat and the sample could be shuttled back and forth between the high pressure reactor and the UHV surface analysis chamber via a special UHV manipulator.

The iron catalysts were prepared by reducing ultra-high purity iron oxide (Fe_2O_3) in an external tube furane. The reduction was carried out to completion at 675K, 1 atm H_2 for 24 hours. The surface of this pyrophoric powder was then passivated for 2 hours in a 1% O_2 in He mixture. The passivated iron powder was characterized by x-ray diffraction and only α -iron was detected. XPS analysis of the same sample revealed only Fe_2O_3 on the surface. These data indicate that the passivated iron powder consists of an iron core surrounded by a thin skin of iron oxide.

2.5 grams of the passivated powder was impregnated with .015 grams of K_2CO_3 through a standard aqueous incipient wetness technique. The surface areas of the two samples (with and without) alkali were determined by the BET method. The potassium containing catalyst had a surface area of $16 \text{ m}^2/\text{gram}$ and the untreated catalyst had a surface area of $18 \text{ m}^2/\text{gram}$. Assuming complete dispersion of the potassium and a surface site density on the iron of $10^{15} / \text{cm}^2$, the potassium coverage on the iron surface is approximately

1/3 of a monolayer.

RESULTS AND DISCUSSIONS

A detailed report on the surface compositional changes that accompany pretreatment and activation of the iron catalysts has been reported elsewhere (10-11). The surface of the untreated iron catalyst consists primarily of iron in +3 oxidation state (Fe_2O_3). Upon reduction (H_2 , 2 atm, 625 K), the surface is converted to metallic iron. The metallic iron surface is, however, unstable under synthesis gas ($H_2:CO$ 3:1, 525 K, 6atm) and is slowly converted to iron carbide. Concomitant with the carbidization of the iron surface is a marked increase in the rate of catalytic reaction of CO to hydrocarbons. Steady state activity is reached after 3-4 hours under reaction conditions. The steady state product distribution of the unpromoted iron carbide surface consists primarily of methane and small linear alkanes. Two types of carbon species were identified on the surface of unpromoted material after reaction. A carbidic form of carbon that was reactive to H_2 and was easily convert to methane. The second type of surface carbon was a coke-like or graphitic deposit that was very unreactive to H_2 . This second type of carbon was found to dominate the surface and poison the reaction when the reaction was run at elevated temperatures.

The surface of the potassium treated catalyst after reduction consisted of a metallic iron with a strongly adsorbed potassium oxygen complex of approximately 1:1 stoichiometry. The stability of this complex is evident since it is formed by decomposition of the thermodynamically stable K_2CO_3 . Upon exposure to synthesis gas the metallic iron is once again converted to iron carbide and a slow increase in reactivity accompanies this change in surface composition. The product distribution over the potassium treated catalyst is substantially different than that observed over the unpromoted surface. The methane yield is lower, the average molecular weight is higher and the product now consists primarily of linear alkenes. After reaction the surface is covered by layer of hydrocarbon which is best characterized as polymethylene.

It has been suggested in the literature that the role of surface alkali in this reaction is to facilitate the dissociation of CO on the surface (9). Presumably, the increased concentration of reactive carbon on the surface shifts the product distribution towards higher molecular weights by enhancing the chain building step in the reaction. However, the results of this study clearly show that the iron and iron carbide surfaces easily break the carbon-oxygen bond in CO. The unpromoted catalyst is saturated in carbon which is reactive towards hydrogen. Therefore, it does not seem reasonable that the role of surface alkali is to enhance CO dissociation. The simple and straight forward explanation of the results of this study is that originally proposed by Dry(2). Potassium addition increases the heat of adsorption of CO and weakens the adsorption of H_2 which in turn changes the relative concentrations of CO and H on the surface of the catalyst under reaction conditions. Our results indicate that the unpromoted iron carbide is a very good hydrogenation catalyst producing primarily small alkanes. Little or no hydrocarbon fragments are observed on the surface after reaction. When potassium is added the overall hydrogenation activity of the surface drops. Larger alkanes dominate the product and there is an accumulation of hydrocarbon

fragments or intermediates on the surface. It appears that the un-promoted surface is too good a hydrogenation catalyst with a high hydrogen activity at the surface. The hydrocarbon intermediates which form on the surface are rapidly intercepted by surface hydrogen and terminated as small alkanes. When potassium is present the hydrogen activity at the surface is much lower, this allows the hydrocarbon intermediates to accumulate and polymerize on the surface and results in larger molecules which are alkenes and not alkanes.

REFERENCES.

1. F. Fischer and H. Tropsch, Ber. Deut. Chem. Ges. B59(1926) 830.
2. M.E. Dry, T. Shingles, L. J. Boshoff and G.J. Oosthuizen, J. Catalysis 15 (1969) 190.
3. J. Benziger and R. J. Madix, Surface Science 94 (1980) 119.
4. K. Subramanzam and M. R. A. Rao, J. Res. Inst. Catalysis Hokkaido 18 (1970) 124.
5. H. Kobel and W.K. Muller, Ber. Bunsenges Physik. Chem. 67 (1963) 212.
6. G. Broden, G. Gafner and H.P. Bonzel, Surface Science 84 (1979) 295.
7. S. R. Kelemen, A. Kaldor and D. J. Dwyer, Surface Science 121 (1982) 303.
8. J. E. Crowell, E. L. Garfunkel and G.A. Somorjai, Surface Science 121 (1982) 303.
9. H. P. Bonzel, Chem. Ing. Tech. 54 (1982) 908.
10. D. J. Dwyer and J. H. Hardenburgh, J. Catalysis 87 (1984) 66.
11. D. J. Dwyer and J. H. Hardenburgh, Appl. Surface Science 19 (1984) 14.

atmosphere. Product gases exiting the cell were analyzed by gas chromatography (temperature programmed Porapak Q column) utilizing a combination of thermal conductivity and flame ionization detection. Following evacuation of the reaction cell, samples could be transferred into the UHV chamber without exposure to air.

The materials characterized included high purity iron foils (Johnson Matthey), and commercially obtained Fe_3O_4 and Fe_2O_3 powders (Alfa Products). Oxide samples were mounted by pressing the powders into 48 mesh copper screen. All synthesis reactions were carried out over the Fe_2O_3 powder, after first reducing the oxide in flowing hydrogen for 9 hours at 400°C. Hydrogen chemisorption measurements, using the method described by Amelse, et al. (12), yielded an uptake of 21 $\mu\text{mole H}_2/\text{g Fe}$ for the reduced powder. Specific reaction rates were calculated based on the hydrogen uptake, assuming two surface iron sites per adsorbed H_2 molecule. Gases used in the sample reductions and synthesis reactions were dried by passage through a silica gel bed immersed in a dry ice/acetone bath. Oxygen impurities were removed by a 10% MnO/SiO_2 trap which had previously been reduced in flowing hydrogen at 350-400°C. The 3:1 H_2/CO synthesis mixture (Matheson) was obtained in an aluminum cylinder to minimize the formation of carbonyls. A silica gel trap heated to 200°C was used to remove any carbonyls present in the reactant stream.

RESULTS

Oxidized Iron Surfaces

The $\text{Fe}(2p)$ XPS spectra characteristic of iron and the stoichiometric oxides are summarized in Figure 1. The metallic iron spectrum (Figure 1a) was measured for a foil sample after the surface had been cleaned by repetitive cycles of argon ion sputtering and annealing at 450°C in the vacuum chamber. The surfaces of the air-exposed oxide powders were invariably contaminated by adsorbed water, as evidenced by broadening on the high binding energy side of the $\text{O}(1s)$ XPS peaks. In the case of the Fe_2O_3 powder, mild heating in vacuum (1 hr at 170°C) removed nearly all of this surface contamination, resulting in the spectrum shown in Figure 1c. The surface of the Fe_3O_4 powder was at least partially oxidized to Fe_2O_3 , based on the $\text{Fe}(2p)$ peak positions and satellite structure measured for as-prepared samples. Using the spectrum fitting procedure described below, we observed that brief (<2 min) argon ion sputtering of iron oxide surfaces results in the reduction of $\text{Fe}(\text{III})$ to $\text{Fe}(\text{II})$, while prolonged sputtering leads to the formation of a significant metallic iron phase. In either case, this surface reduction is accompanied by a decrease in the ratio of the oxygen to iron XPS intensities. The Fe_3O_4 spectrum (Figure 1d) was obtained for a powder sample after brief argon ion sputtering, followed by heating for 5 hours at 350°C in vacuum. During this sample heating, the $\text{O}(1s)/\text{Fe}(2p3/2)$ intensity ratio increased steadily and then leveled off, signaling a gradual re-oxidation of the sputtered surface.

In a recent review of oxide photoemission studies, Wandelt (13) observed that the $\text{Fe}(2p)$ XPS spectrum of Fe_3O_4 is simply a weighted average of the spectra for Fe_2O_3 ($\text{Fe}(\text{III})$) and Fe_xO (primarily $\text{Fe}(\text{II})$). This is illustrated by the $\text{Fe}(\text{II})$ spectrum in Figure 1b, which was obtained by subtracting out the $\text{Fe}(\text{III})$ contribution to the Fe_3O_4 spectrum (assuming an $\text{Fe}(\text{III})$ to $\text{Fe}(\text{II})$ area ratio of 2:1). The resulting $\text{Fe}(\text{II})$ peak positions and satellite structure are in excellent agreement with XPS results reported for Fe_xO (13, 14).

Spectra representing the individual oxidation states of iron (Figure 1a,b,c) can be used to analyze data obtained for partially oxidized surfaces, as illustrated in Figure 2. The points in this figure indicate data measured for an iron foil after brief exposures to 1×10^{-6} torr of oxygen at 400°C. The solid curves through these points indicate linear combinations of the spectra representing the individual iron oxidation states. Coefficients for these linear combinations were determined using the usual least squares minimization criteria. The individual contributions of each oxidation state to the fitted spectra are also indicated in Figure 2. This procedure allows the compositions of partially oxidized surfaces to be approximated in terms of the area contributions of each oxidation state to the total XPS spectrum. Area contributions to the spectra in Figures 2a and 2b are 78% Fe / 7% Fe(II) / 15% Fe(III), and 23% Fe / 29% Fe(II) / 48% Fe(III), respectively.

Carbided Iron Surfaces

Iron carbides were prepared by treating reduced powder samples either with ethylene or a 3:1 H₂/CO mixture at 250–275°C. Analysis of these samples by Mössbauer spectroscopy indicated that the powders were fully carburized and consisted primarily of X-Fe₅C₂. XPS results for the carbide powders did not depend on the carburization medium employed, and we therefore limit discussion in this section to samples carbided under normal synthesis conditions (250°C, 1 atm, 3:1 H₂/CO).

The catalytic behavior of the initially reduced powder is illustrated in Figure 3. The turnover frequency for methane formation increased steadily during the first 4 hours of synthesis and then remained nearly constant at ~0.0035 molecules/site sec for times in excess of 20 hours. The steady state turnover frequency compares well with values in the range of .003 to .007 molecules/site sec reported by Amelse, et al. (12) for silica supported iron under similar reaction conditions. The steady state CO conversion level over the iron powder catalyst was 0.6%, based on integration of the C₁ to C₅ hydrocarbon products. Analysis of the hydrocarbon product distribution by the Schulz-Flory model yielded a chain growth parameter $\alpha = 0.48$.

XPS results obtained for the iron powder in the reduced and fully carburized states are summarized in Figure 4. The reduced catalyst exhibited an Fe(2p_{3/2}) binding energy of 707.0 eV, and a shift to 707.3 eV was observed following exposure to synthesis conditions for 30 hours. Dwyer and Hardenbergh (15) reported a similar shift upon carburization of unsupported iron during low conversion synthesis at 7 atm. In addition to small increases in the iron core level binding energies, the metal and carbide phases are distinguished by differences in the iron Auger line shape, as illustrated in Figure 4. The most pronounced difference in line shape occurs for the Fe(LMV) Auger transition, in the kinetic energy range from 610 to 660 eV. When Al K_α x-rays are used, this region also includes the Fe(2s) core level transition at a kinetic energy of ca. 639 eV.

Since the Fe(2p_{3/2}) peaks of metallic iron and X-Fe₅C₂ are nearly identical in shape and differ in position by only 0.3 eV, changes in the iron Auger spectrum provide a more useful method for characterizing mixtures of these phases. This is demonstrated by the results in Figure 5, which were obtained for a reduced powder sample after exposure to synthesis conditions for periods of 20 and 100 minutes. The Auger spectra in this figure were fit with linear combinations of the metal and carbide spectra (Figure 4), using the

least squares method described earlier. Area contributions of the carbide phase to the iron Auger spectra were 36% and 48% after synthesis for 20 and 100 minutes, respectively. The C(1s) spectra in Figure 5 illustrate the utility of XPS in characterizing the carbon adlayer which develops on catalyst surfaces during the Fischer-Tropsch synthesis. Krebs, et al. (9) have shown that the initial increase in activity observed during synthesis over iron foils is associated with the formation of surface "carbidic" carbon, corresponding to the low binding energy (283.2 eV) C(1s) peaks in Figure 5. The high binding energy (285.3 eV) peaks in these spectra indicate the presence of graphitic surface carbon, which is associated with the deactivation of iron synthesis catalysts.

CONCLUSIONS

Analysis of Fe(2p) XPS and iron Auger spectra, combined with C(1s) XPS measurements, provides a valuable technique for studying the compositional behavior of Fischer-Tropsch catalysts. The extent of catalyst oxidation during synthesis at high conversions may be estimated in terms of the area contribution of oxide phases to the Fe(2p) spectrum. Similarities between the metal and carbide core level spectra are likely to complicate the determination of these phases when oxides are present. Analysis of the metal and carbide contributions to the iron Auger spectrum provides an alternate method for monitoring surface carbide formation during low conversion synthesis. The "surface compositions" obtained in this manner are at best semi-quantitative, since the contribution of a particular phase to the XPS or Auger spectrum will depend on both the amount and distribution of that phase within the detected volume. In spite of this, the spectrum fitting technique should prove to be useful in characterizing the time and conversion dependent nature of the active catalyst surface.

REFERENCES

- (1) J.A. Amelse, J.B. Butt, and L.H. Schwartz, *J. Phys. Chem.*, 82, 558 (1978).
- (2) G.B. Raupp and W.N. Delgass, *J. Catalysis*, 58, 348 (1979).
- (3) K.M. Sancier, W.E. Isakson, and H. Wise, *Adv. Chem. Ser.*, 178, 129 (1979).
- (4) J.W. Niemantsverdriet, A.M. van der Kraan, W.L. van Dijk, and H.S. van der Baan, *J. Phys. Chem.*, 84, 3363 (1980).
- (5) G.B. Raupp and W.N. Delgass, *J. Catalysis*, 58, 361 (1979).
- (6) H. Matsumoto, *J. Catalysis*, 86, 201 (1984).
- (7) J.F. Shultz, W.K. Hall, B. Seligman, and R.B. Anderson, *J. Amer. Chem. Soc.*, 77, 213 (1955).
- (8) R.B. Anderson, L.J.E. Hofer, E.M. Cohn, and B. Seligman, *J. Amer. Chem. Soc.*, 73, 944 (1951).
- (9) H.J. Krebs, H.P. Bonzel, and G. Gafner, *Surf. Sci.*, 88, 269 (1979).
- (10) H.P. Bonzel and H.J. Krebs, *Surf. Sci.*, 91, 499 (1980).
- (11) H.J. Krebs and H.P. Bonzel, *Surf. Sci.*, 99, 570 (1980).
- (12) J.A. Amelse, L.H. Schwartz, and J.B. Butt, *J. Catalysis*, 72, 95 (1981).
- (13) K. Wandelt, *Surf. Sci. Reports*, 2, 1 (1982).
- (14) M. Oku and K. Hirokawa, *J. Appl. Phys.*, 50, 6303 (1979).
- (15) D.J. Dwyer and J.H. Hardenbergh, *J. Catalysis*, 87, 66 (1984).

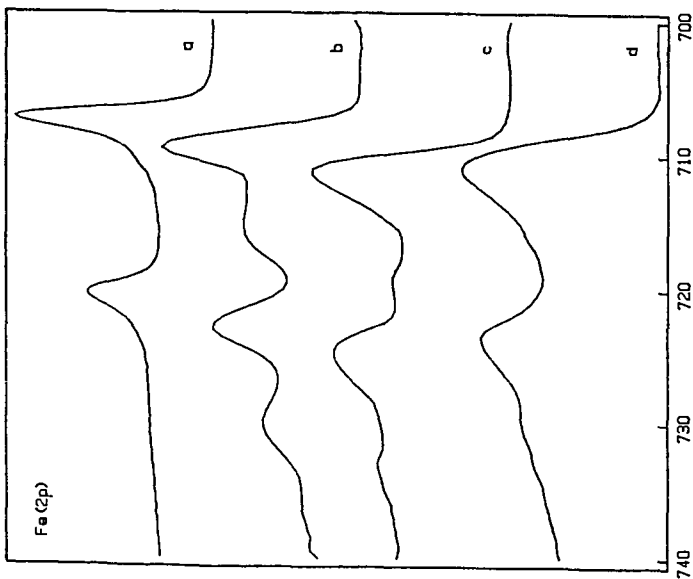


Figure 1. Fe(2p) XPS spectra of metallic iron and iron oxides. (a) clean foil
 (b) Fe(II) contribution to Fe_3O_4
 spectrum (c) Fe_2O_3 (d) Fe_3O_4 .

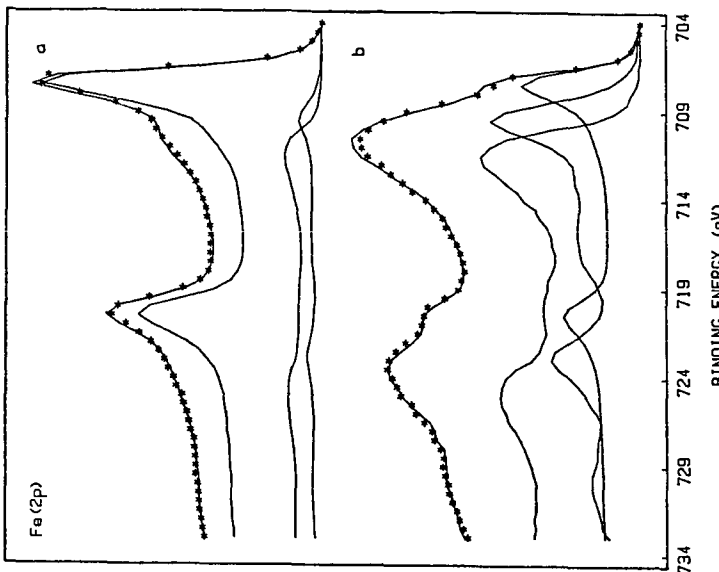


Figure 2. Examples of Fe(2p) spectrum fitting
 for partially oxidized iron foil.
 (a) 170 L O_2 (b) 670 L O_2 at 400°C .

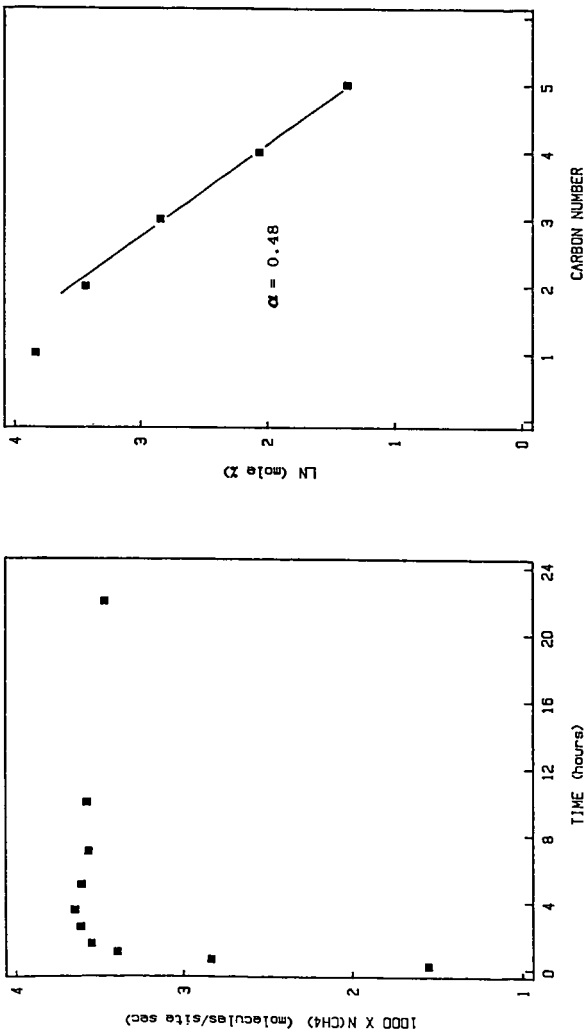


Figure 3. Methane turnover frequency versus time and steady state Schulz-Flory plot for synthesis over unsupported iron powder (250°C, 1 atm, 3:1 H₂/CO).

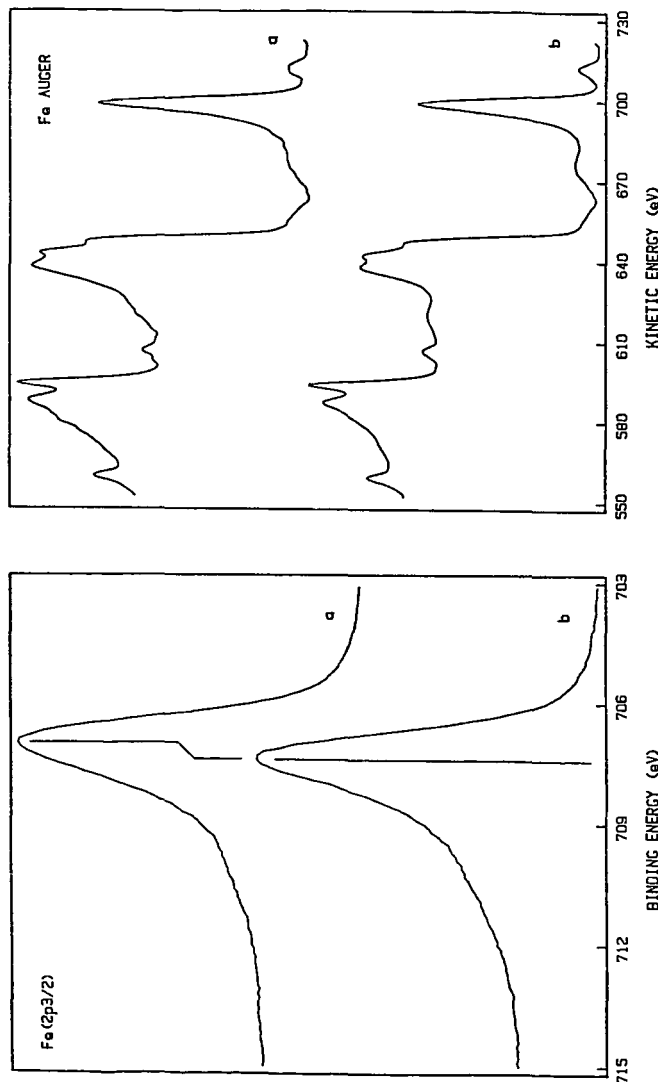


Figure 4. Fe(2p_{3/2}) XPS and Fe Auger spectra of unsupported iron powder.
 (a) after reduction in 1 atm H₂ at 400°C (b) after hydrocarbon synthesis for 30 hr in 1 atm 3:1 H₂/CO at 250°C.

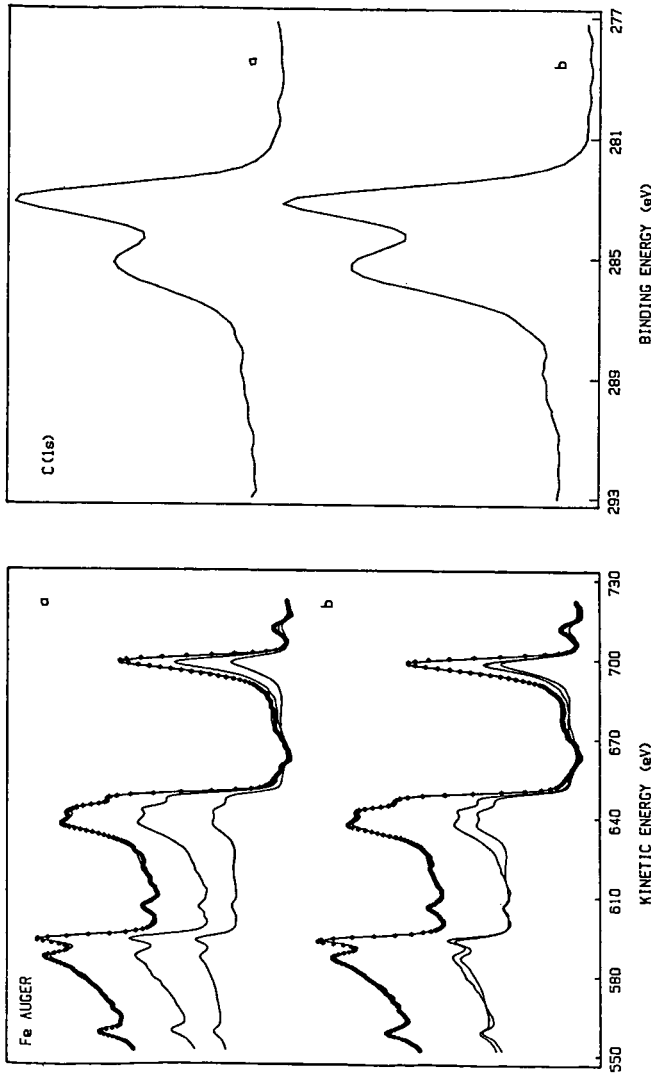


Figure 5. Fe Auger and C(1s) XPS spectra of unsupported iron powder after hydrocarbon synthesis for (a) 20 min (b) 100 min. Fe Auger spectra area contributions are: (a) 64% metal, 36% carbide (b) 52% metal, 48% carbide.